# Spatial-temporal dynamics of chaotic behavior in cultured hippocampal networks

Wenjuan Chen, Xiangning Li,[*,†] Jiangbo Pu, and Qingming Luo[*,‡]
*Britton Chance Center for Biomedical Photonics, Wuhan National Laboratory for Optoelectronics, Huazhong University of Science and Technology, Wuhan, Hubei 430074, China*
(Received 17 November 2009; revised manuscript received 25 March 2010; published 1 June 2010)

Using multiple nonlinear techniques, we revealed the existence of chaos in the spontaneous activity of neuronal networks *in vitro*. The spatial-temporal dynamics of these networks indicated that emergent transition between chaotic behavior and superburst occurred periodically in low-frequency oscillations. An analysis of network-wide activity indicated that chaos was synchronized among different sites. Moreover, we found that the degree of chaos increased as the number of active sites in the network increased during long-term development (over three months *in vitro*). The chaotic behavior of the dissociated networks had similar spatial-temporal characteristics (rapid transition, periodicity, and synchronization) as the intact brain; however, the degree of chaos depended on the number of active sites at the mesoscopic level. This work could provide insight into neural coding and neurocybernetics.

DOI: 10.1103/PhysRevE.81.061903 PACS number(s): 87.18.−h, 87.10.−e, 87.85.−d, 87.80.−y

## I. INTRODUCTION

Understanding the coding and organization mechanisms of nervous system presents a great challenge to investigators in both neuroscience and information science [1,2]. Recent developments in nonlinear science show that nonlinear techniques are well-suited for studying the mechanism underlying the irregular activity of neural networks [3–5]. As a famous nonlinear phenomenon, chaos is defined as highly disordered dynamics governed by a deterministic system causing unpredictability over a long time period [6]. There are obvious benefits to using chaotic systems, rather than stochastic systems, when describing the complicated characteristics of brain function [7,8]. For instance, the brain's agility when confronted with changing conditions could be explained by the initial sensitivity of chaos. It is widely believed that chaos is critical to consciousness as well as memory storage and retrieval [9,10].

Previous studies have determined the existence of chaos in both signals acquired from isolated or paired neurons and electroencephalograms (EEGs) recorded from large-scale cortical networks [11]. However, neural coding mechanisms that underlie the generation and evolution of chaotic dynamics remain unclear. Because the properties of complete neural networks cannot be represented by simply multiplying single cells, it is difficult to determine the dynamics of an intact brain using only results at the microscopic level. Likewise, neural activity at the macroscopic level is overwhelmingly complex and with inevitable disturbances (e.g., the behavioral drives of animals).

Experiments focusing on different scales and hierarchies of neural organization, such as the mesoscopic level (consisting of hundreds to thousands of neurons), are bridging the gap between theoretical models and actual neural activity [12,13]. Multielectrode array (MEA) allows long-term investigation of neural networks without notable invasion to cells [14]. Neuronal networks cultured on MEA enable more detailed observations and manipulations [15], providing an efficient platform to study neural dynamics at the mesoscopic level. A number of researchers have attempted to understand the complex patterns exhibited by cultured networks during development, including random spike, burst, superburst (also called episode or avalanche), and so on [16–18]. Nonlinear analyses have also been attempted in recent years [19–22], but no chaotic behavior has been determined in the noisy spontaneous activity. Further studies are needed to study the complicated dynamics of neuronal networks *in vitro*.

This study incorporates several analyses of chaotic behavior using the interspike interval (ISI) series from long-term cultures. Within this series, we measure the correlation dimension, calculate the largest Lyapunov exponent, and apply surrogate data techniques. After further analysis of the network's spatial-temporal characteristics, we demonstrate an emergent change in chaotic firings and a correlation between the degree of chaos and the number of active neurons.

## II. MATERIALS AND METHODS

### A. Neuronal cultures

Experiments were approved by the Regulations for the Administration of Affairs Concerning Experimental Animals in Hubei Province. Hippocampal cells were dissociated from the brains of embryonic day 18 rats. After enzymatic digestion, cells were separated by trituration. Fifty thousand cells were planted in a 20 $\mu$l drop of culture medium on a MEA, forming a dense monolayer. The dishes were flooded with 1 ml of medium after the cells had adhered to the substrate (more than 30 min) and stored with FEP membrane lids in an incubator at 37 °C and 5% $CO_2$. The medium was half changed twice per week. More details are provided in our earlier publications [23,24].

### B. Data collection and preprocess

Electrical activity was recorded with a multielectrode array system (MEA1060 System, MCS GmbH, Germany) con-

*Author to whom the correspondence should be addressed. FAX: +86-27-87792034.
†ibp.hust@gmail.com
‡qluo@mail.hust.edu.cn

 

sisting of multielectrode array dishes, an amplifier (MEA1060), a temperature controller and a data acquisition card controlled by MC_RACK software. The multielectrode array dish had 60 substrate-embedded titanium nitride electrodes in an $8\times8$ layout grid with electrode diameters of 30 $\mu$m and interelectrode distances of 200 $\mu$m. After $1200\times$ amplification, signals were sampled at 25 kHz. For each channel, the threshold for spike detection was set at five standard deviations (SDs) from the average noise amplitude during the first 500 ms of each measurement. Spike sorting was not used in this experiment because there is no consensus on the accuracy of this technique and its employment would have critically influenced all subsequent analyses [25,26]. Raster plots and burst detection were implemented using Neuroexplorer (Nex Technologies, Littleton, MA, USA). A maximum interval algorithm was performed to identify burst, which was defined as three or more consecutive spikes with interspike intervals of less than 10 ms [27].

### C. Data analysis

#### *1. Chaotic time series analysis*

Based on the reconstruction theory [6], phase space could be reconstructed from the scalar time series {Xn}:

$$X_i = [x_i x_{i+1} \cdots x_{i+(m-1)t}] \quad i = 1,2,N-(m-1), \tag{1}$$

where $N$ was the length of the time series, $t$ was the delay time, and $m$ was the embedding dimension. For discrete time series, the delay time was set as 1 [6]. The correlation integral of the embedded time series was defined as [8]

$$C(r) = \frac{2}{M(M-1)} \sum_{1\le i<j\le M}^{n} \theta(r - \|X_i - X_j\|)$$
$$M = N-(m-1), \tag{2}$$

where $\theta$ was the Heaviside function. The correlation dimension quantifying the self-similarity of attractor was given by the slope of ln $C(r)$ versus ln $r$. If the correlation dimension became saturated with increasing $m$, the system represented by the time series should possess a chaotic attractor [28].

The largest Lyapunov exponent ($\lambda$) is another widely used measure to quantify the degree of chaos. According to the method proposed by Rosenstein *et al.* [29], it can be calculated by tracking the exponential divergence $d_j(i)$ of the nearest neighbors:

$$d_j(i) = d_j(0)e^{\lambda(i\Delta t)}. \tag{3}$$

A positive $\lambda$ is usually taken as a strong signature of chaos [3,30].

The significance of $\lambda$ was tested with surrogate data generated by two standard techniques [31]: (i) random shuffling of the data and (ii) phase randomization of the Fourier spectrum. *U*-test was chosen to determine whether the irregularity of the ISI series was due to nonlinear determinism or random noise of the neuronal networks [32]:

$$S = \frac{|q_0 - E(q_{surr})|}{\sigma_{surr}}, \tag{4}$$

where $q_0$ was the statistical value of the original data, while $E(q_{surr})$ and $\sigma_{surr}$ represented the averaged value and standard error of the mean (SEM) of the surrogate data, respectively. The experimental data could be distinguished from random noise if $S$ was larger than 1.96.

To increase the credibility of the observed chaos in the experimental time series, three other statistical measurements of nonlinearity were applied to the surrogate data.

(1) Time reversibility [6]

$$T_r = \frac{E(x_n - x_{n-\tau})^3}{(E(x_n - x_{n-\tau})^2)^{3/2}}. \tag{5}$$

$T_r$ was a measure of efficiency introduced to quantify the asymmetry of the time series under conditions of time reversal, as the linear stochastic process was always symmetrical under these conditions.

(2) High-order moment [31,33]

$$T_c = \frac{E(x_n x_{n-\tau} x_{n-2\tau})}{|E(x_n x_{n-\tau})^{3/2}|}. \tag{6}$$

$T_c$ denoted the degree of time asymmetry, a strong signature of nonlinearity.

(3) Local variation [5,34]

$$L_v = \frac{3}{N-1} \sum \frac{(x_n - x_{n+\tau})^2}{(x_n + x_{n+\tau})^2}. \tag{7}$$

$L_v$ extracted intrinsic irregularity in the spike trains.

The variable $x$ and $\tau$ in the above equations represented the normalized ISI series and time delay, respectively. To perform chaotic time series analysis, the TSTOOL1.2 software package was used (http://www.physik3.gwdg.de/tstool/).

#### *2. Network activity analysis*

Only spike trains recorded from active electrodes (electrodes with a mean firing rate greater than 1 Hz) were used to calculate the network-wide firing rate and the coefficient of variation,

$$C_v = \frac{\sigma_{ISI}}{E_{ISI}}. \tag{8}$$

A transition state was considered to have occurred when the rate of change ($R_c$) of both the firing rate and the $C_v$ were larger than 30%. The minimum duration of each state was set at 20 s;

$$R_c = \frac{|x_{n+1} - x_n|}{x_n} \times 100\%. \tag{9}$$

Nonlinear linkage between different electrodes was measured by mutual information [35], which was calculated using the CRP toolbox (http://tocsy.pik-potsdam.de/):

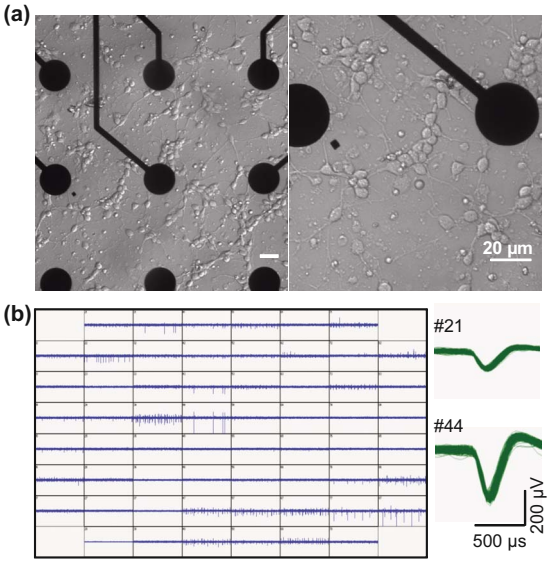


FIG. 1. (Color online) Neuronal networks cultured on multielectrode array. (a) Hippocampal neurons cultured on multielectrode array (21 DIV). The black solid circles are electrodes separated by 200 $\mu$m with diameters of 30 $\mu$m. Scale bar, 20 $\mu$m. (b) Spontaneous activity of the entire cultured network.

$$M(x,y) = \sum_i p_i(x)\ln p_i(x) + \sum_j p_j(y)\ln p_j(y) - \sum_{i,j} p_{i,j}(x,y)\ln p_{i,j}(x,y). \quad (10)$$

Spike trains with significant peaks were considered to be related [35] when the peak value was larger than an appointed threshold ($3\times$SD).

As an effective measure of neural synchronization at the network level, network burst (NB) was detected using the following criterion [36]. First, the total spike counts of active sites in consecutive time bins (25 ms) were calculated; a network burst was considered to have occurred when this value exceeded an appointed threshold ($3\times$mean firing rate per bin). Then the time at the exact center and boundary of each network burst were identified before averaging. Finally, we used statistical parameters of network burst (mean rate, peak value, duration, and spike in network burst) to characterize neural synchronization.

## III. RESULTS

The hippocampal neurons began neurite outgrowth within several hours and organized into a network after a few days *in vitro* (DIV). The spontaneous activity of the cultured networks was recorded from the first week until at least the twentieth week *in vitro*. The firing patterns took on various transitions during development. As shown in Fig. 1, neural signals were measured simultaneously from 60 electrodes surrounded by one or more neurons for 21 DIV. The temporal patterns varied greatly between different sites in the networks. For example, there were random spikes with small amplitudes at some sites, while other sites alternated spikes and bursts.

TABLE I. Characteristics of the spontaneous activity including superburst and chaotic behavior.

| MEA No. | Days *in vitro* | Firing rate (Hz/s) | NB frequency (Hz/s) |
|---|---|---|---|
| 6200[a] | 27 | 142.35 ± 3.67 | 1.36 |
| n1240[a] | 57 | 1101.78 ± 27.66 | 1.63 |
| n1253[a] | 49 | 797.32 ± 24.92 | 1.25 |
| n1029[a] | 32 | 311.79 ± 10.03 | 1.34 |
| n1271 | 36 | 941.61 ± 15.32 | 1.37 |
| 6195 | 26 | 83.60 ± 2.88 | 0.53 |
| n1262 | 55 | 250.45 ± 7.82 | 0.73 |
| n1273 | 41 | 92.70 ± 4.98 | 0.67 |
| n1270 | 32 | 334.99 ± 10.07 | 1.60 |
| n1258 | 34 | 544.80 ± 20.38 | 1.13 |

[a]The cultures were recorded in long term (117, 129, 156, and 218 days *in vitro*, respectively).

Superburst was observed after two weeks *in vitro* and dominated the network activity during the next two weeks. In later stages (about 4–9 weeks *in vitro*), a unique phenomenon was found in more than ten cultures (the details are shown in Table I). As an example of this phenomenon, the waveforms of the spike train recorded from one electrode are shown in Fig. 2(a). Two distinct layers are clearly shown in the scatter plot of ISIs [Fig. 2(b)], indicating a period when the neural networks displayed a cluster of bursts with an increasing interburst interval. This activity resembles the interesting nonlinear phenomenon of bifurcation, which is an important criterion for assessing chaos in theoretical results [8]. For this reason, we used first return map to analyze the irregular firings that appeared after the superburst. There was no deterministic structure, such as a one-hump shape, in the

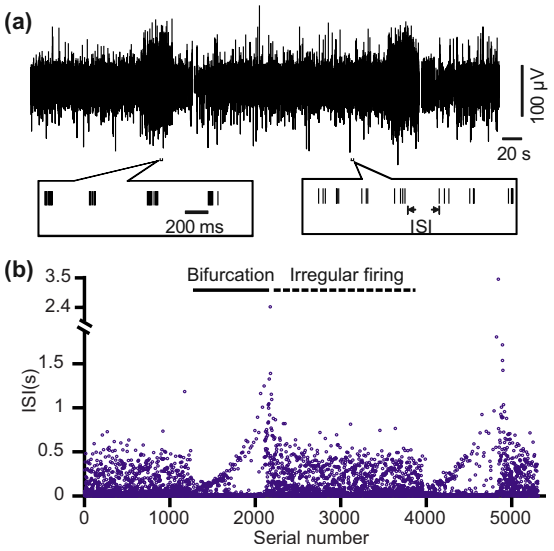


FIG. 2. (Color online) Bifurcation in the spontaneous ISI series. (a) The spontaneous spike train of 500 s recorded from a single site (DIV=32). Each line in the raster plot represents a spike detected from background noise. (b) Irregular ISIs emerged from an obviously bifurcated background.

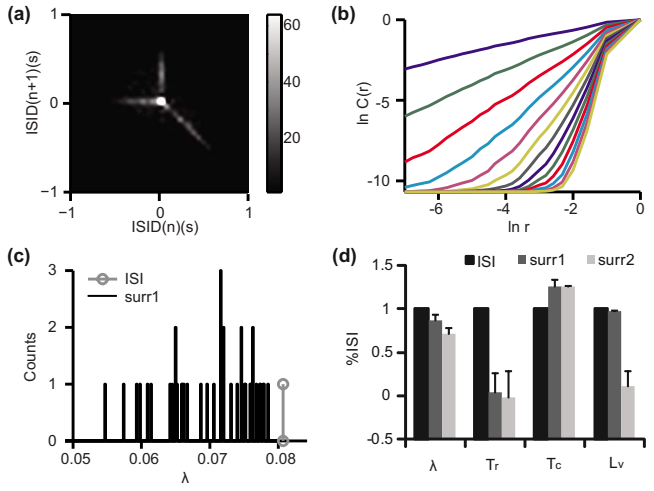


FIG. 3. (Color online) Chaotic time series analysis of the irregular ISI series. (a) The first return map of ISID. The color bar on the right corresponds to the number of points that fell into each cell. The size of each cell was 50 ms × 50 ms. (b) The correlation integral curves at a log-log scale were convergent with increasing embedding dimension m (1, 2, 3, …, 13 from top to bottom). (c) Histogram of the largest Lyapunov exponents, bin=0.001. 40 surrogate data sets (black line) were generated by shuffling the original ISI series (gray line with circle). (d) Hypothesis test of four nonlinear statistics, including the largest Lyapunov exponent (λ), time reversibility ($T_r$), high-order moment ($T_c$), and local variation ($L_v$). Two different surrogate data techniques (Surr1 for shuffling samples and Surr2 for permuting Fourier) were applied, and 40 groups of surrogate data sets were generated in each test.

first return map of ISI [37]. However, a recognizable "*Y*" structure was clearly shown in the interspike interval difference [ISID, $\mathrm{ISID}(n)=\mathrm{ISI}(n+1)-\mathrm{ISI}(n)$] return map [Fig. 3(a)], a structure quite different from the triangle structure without any preferred subpatterns in random firing [38]. The irregular firings after the superburst could thus not be stochastic; instead, they suggest deterministic chaos.

### A. Chaotic behavior in the spontaneous activity of hippocampal networks

To determine whether the irregularity of neural activity was governed by a deterministic mechanism, both direct metrical quantities (correlation dimension and the largest Lyapunov exponent) and an indirect tool (surrogate data) of chaotic time series analysis were applied to the irregular ISIs. The analysis of correlation dimension is shown in Fig. 3(b). The correlation integral curves on a log-log scale were convergent with the embedding dimension as it increased to 13, but the linear zone was difficult to distinguish. The result seemed to be affected by noise or the limited length of neural signals [11], both of which were inevitable in our experiments.

The largest Lyapunov exponent of the irregular ISI series was then calculated. Even if the result (λ=0.0807) suggested the existence of chaos, we hesitated to draw conclusions because of noise. Therefore, surrogate data techniques were applied to test the significance of λ. As shown in Fig. 3(c), the λ was significantly larger of the original ISI series than of the surrogate data which was generated by shuffling ISI series ($S=10.90$). Similar result was observed when randomizing the phase of the Fourier spectrum ($S=25.24$).

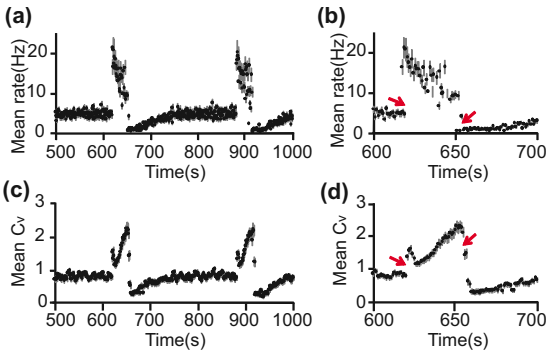


FIG. 4. (Color online) Sudden transition between superburst and chaotic firing. (a) Mean firing rate (circle) ± SEM (gray line) of all active sites, bin=1 s. (b) Partial enlarged view of the left figure indicating sudden changes in the spontaneous firing rate between bifurcation and chaos. (c) and (d) display the curves of correlation variation with an overlapping sliding window (window width =5 s, sliding window=1 s); these curves show sudden transitions between different stages.

To reduce the influence of our selection of variables in the surrogate data test, three other nonlinear statistic tests, including time reversibility, higher-order moment, and local variation, were calculated by cross-linking the two surrogate data techniques. The bar charts show that the original data were remarkably different from the surrogate sets [Fig. 3(d)]. Consequently, we demonstrated chaotic behavior in the spontaneous activity of hippocampal networks *in vitro*.

### B. Temporal evolution of chaotic behavior

The above-mentioned results indicating chaos seemed to be related to superburst, but how did the transition between these two firing patterns emerge? To answer that question, we explored the evolution of the mean firing rate and $C_v$ of the entire network. Figure 4 shows an emergent jump in both firing rate ($R_c=252.60\%$) and $C_v$ ($R_c=69.63\%$) from chaos to bifurcation. At the later transition from bifurcation to chaos, an emergent decrease in both rate ($R_c=79.51\%$) and $C_v$ ($R_c=31.84\%$) occurred. The results showed an emergent transition between superburst and irregular chaotic firing without external input.

Using continuous recording, we found that the transition state seemed to be reversible in all the samples we observed (Fig. 5). By analyzing the network activity for 1000 s, a regular steplike increment in the cumulative burst number curve was observed [Fig. 5(b)], implying that the transition was periodic. A comparison of different chaotic stages indicated no significant differences in either mean firing rate or nonlinear characteristics ($P>0.05$, paired $t$ test, $\alpha=0.05$). These results demonstrated that superburst and chaotic firing recurred alternately throughout the spontaneous activity of the entire culture.

### C. Spatial distribution of chaotic behavior in the network

To analyze the spatial characteristic of the chaotic behavior in the neural network, mutual information was applied to

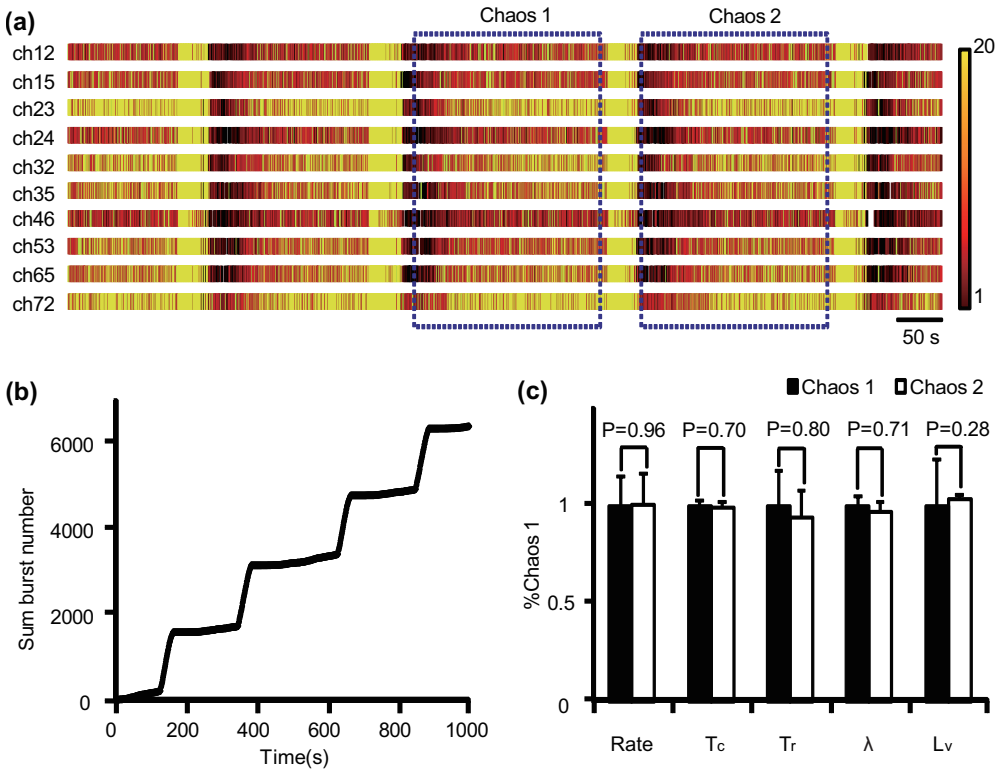


FIG. 5. (Color) Periodic chaos recurred with a series of bursts. (a) Raster plots of spontaneous activity in 1000 s. The site index is indicated at the left of each trace. (b) Cumulative burst number versus time demonstrating a steplike trend. (c) Comparison of network-wide nonlinear statistics at different chaotic stages. The data were presented as the mean ± SEM of active sites in the network and normalized by the value of the first chaotic stage. The *t*-test results indicated that there was no significant difference between two chaotic stages.

quantify the degree of nonlinear correlation between spike trains recorded from different electrodes [ch35 and ch65 were chosen as an example in Fig. 6(c)]. Significant peaks that indicated dependence between different electrodes were observed during both bifurcation and chaos stages. However, the peak value of mutual information in the chaos stage ($M=0.1289$) was much lower than the bifurcation stage ($M=0.2531$), a result in accordance with the results from network burst analysis [Fig. 6(d)]. Except for duration, other network burst parameters (peak value, rate, and spikes in network burst) fell rapidly from the bifurcation to the chaos stage ($P<0.05$, paired *t*-test, $\alpha=0.05$). The synchronous activity of the network underwent an apparent change in its spontaneous state without external disturbance.

Finally, we focused on the spatial distribution of chaotic behavior that presented network-wide synchronization. Because the chaotic time series analysis of several ISIs was not credible, the nonlinear statistics from several electrodes with less than 500 spikes produced values quite different from other electrodes (e.g., $\lambda=0$). Well agreement between the mean firing rate and the largest Lyapunov exponent was found at most of the active sites [Figs. 7(a) and 7(b)].

Further analysis of chaotic behavior in four long-term cultures (with 117, 129, 156, and 218 DIV, respectively) are shown in Fig. 7(c). In each example, the number of chaotic electrodes and the largest Lyapunov exponent (mean ± SEM) were calculated. Interestingly, there was a significant positive correlation between the size and the degree of chaos of the entire network ($R^2=0.6392$ using the linear least-squares method). In summary, our results suggested that the topology of cultured neural networks may influence the degree of chaotic behavior.

## IV. DISCUSSION

In the present study, we investigated the spatial-temporal dynamics of chaotic behavior in the spontaneous activity of cultured hippocampal networks. In previous studies, chaos has been observed by either using the activity of a single neuron after stimulation or pharmacological exposure or examining a neural network *in vivo* under learning and sleep states [3–5,39]. The theory underlying these neural mechanisms remains far from complete [13] because of the enormous gap between the local behavior of neurons and the global state of neural networks *in vivo* (e.g., the rat cerebral cortex, which consists of about $21\times10^{-6}$ neurons) [40].

Cultured neuronal networks at the intermediate mesoscopic level not only expressed more diverse dynamics than single neurons [9,10,12] but also had simpler neural connections than the intact brain and slice [41]. With high accessibility to observation and manipulation, such *in vitro* models may shed light on the role of nonlinear behavior in brain function.

A few pioneers have already used nonlinear measurements to analyze the electrical activity of cultured neuronal networks [19–22]. However, the existence of chaotic behavior has not been previously reported because it is difficult to determine "true" chaos in experimental data [6]. To over-

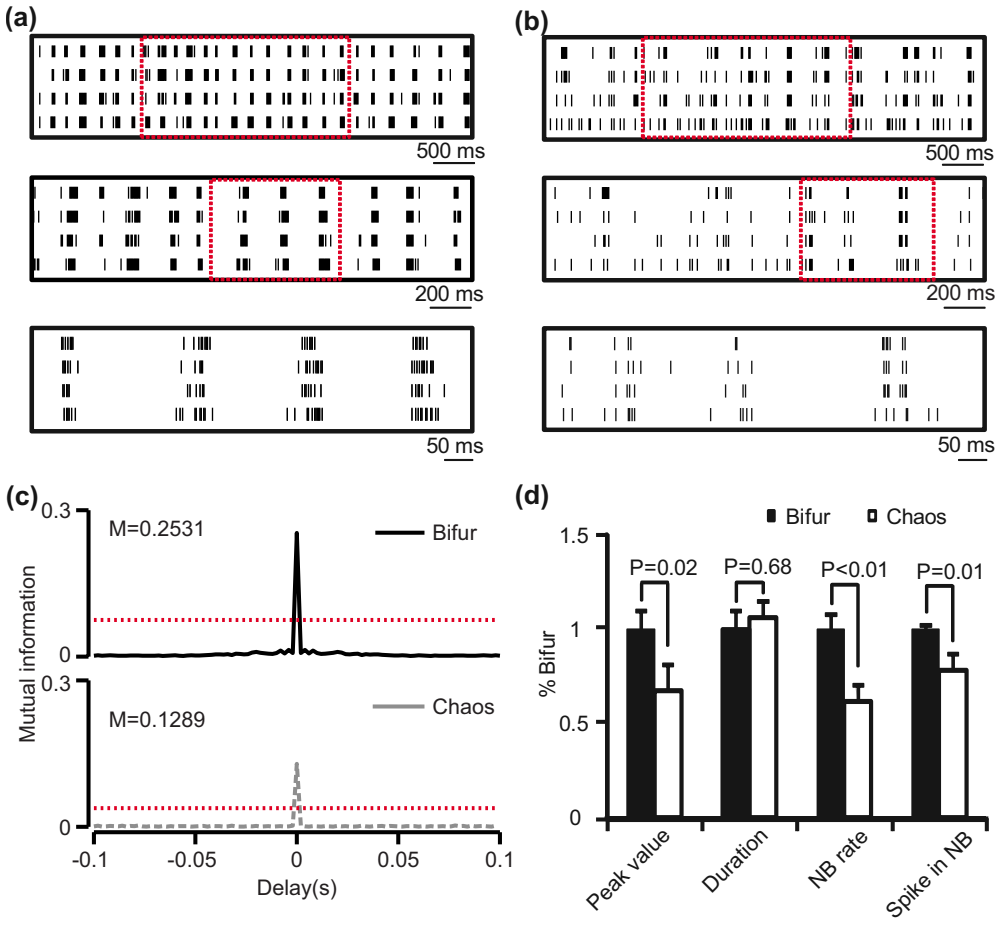


FIG. 6. (Color online) Synchronization of chaos in neural network *in vitro*. (a) Raster plots of spontaneous activity in the bifurcation stage recorded from four electrodes (ch35, ch53, ch65, and ch72 from top to bottom). At the bottom of each raster, the time scale bar is shown. (b) Raster plots of spontaneous activity in the chaos stage were recorded from the same electrodes shown in the graph (a). (c) Mutual information between ch35 and ch65 (solid black line for bifurcation and dashed gray line for chaos). The threshold for detecting a significant peak was defined as $3 \times \mathrm{SD}$ (dotted line). (d) Comparison of network bursts detected in the bifurcation and chaos stages (mean $\pm$ SEM); *P*-value was calculated using a paired *t*-test ($\alpha$=0.05).

come such difficulties, we applied more sophisticated and rigorous quantification procedures (determining correlation dimension, calculating the largest Lyapunov exponent, and using surrogate data) to determine chaotic behavior. The original ISI series was significantly different from random signals (Fig. 3). In addition, our previous studies showed that the spontaneous activity of hippocampal networks on MEA can be recorded from 60 electrodes simultaneously in a long term (more than 20 weeks *in vitro*) [23]. This finding prompted us to observe more diverse dynamics using a large and detailed collection of neuroscientific data. In this work, we demonstrated an activity pattern (deterministic chaos) in cultured networks, a result that may assist in developing models of neural networks.

In contrast to the many studies that demonstrate chaos in neural activity [8,11], fewer studies have focused on the temporal evolution of chaotic behavior in neural networks. The present study showed emergent changes between chaotic firing and superburst that occurred periodically without external disturbance (Fig. 4). Following earlier studies, the transitory dynamics was regarded as chaotic itinerancy [10,39,42]. Because chaotic itinerancy facilitates rapid responses to any stimulus, our work may be helpful in the field of neurocybernetics, allowing the development of intelligent artificial limbs that directly interface with the nervous system. Moreover, neural activity in different stages had similar characteristics (Fig. 5). The cultured networks repeated these transitory dynamics, a behavior different from the hippocampal slice cultures [42]. This finding may benefit from sufficient length of multielectrode recording. Because the periodic alternation of chaotic attractor and other states (e.g., limit cycle) is believed to play an important role in episodic memory [43], our study could provide insight into plasticity and learning at the network level.

Information processing in living organisms is often determined by the structure of neural networks [41,44]. How are dissociated neurons efficiently constructed into a complex network with nonlinear dynamics? Chaotic synchronization, a crucial neural behavior that facilitates the transmission and coordination of neural information among various brain areas [45], was found in cultured hippocampal networks (e.g., significant peaks of mutual information in Fig. 6). Because chaos is excessively sensitive to initial conditions, chaotic synchronization should be formed by coupled oscillators but

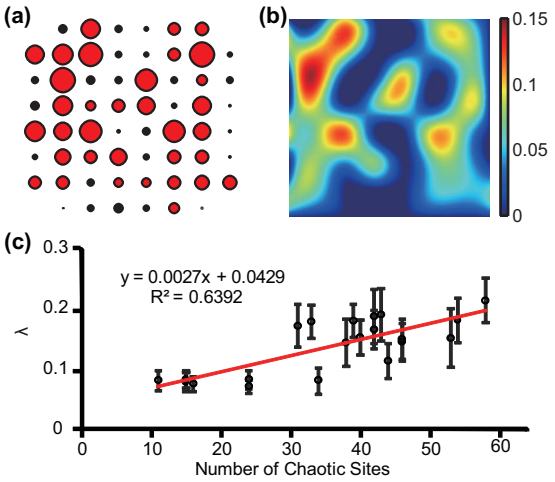


FIG. 7. (Color) Spatial distribution of chaotic behavior. (a) Mean firing rates of spontaneous chaos firing. Each circle whose diameter was plotted using mean firing rate corresponds to a single electrode. (b) Spatial distribution of the largest Lyapunov exponent in the network (smoothed using the spline function). (c) Scatter plot of the number of chaotic sites versus the largest Lyapunov exponent showing a significant positive correlation. The line was fitted using the linear least-squares method.

not spike coincidence. The network-wide synchronization of chaos in the spontaneous activity implies that neurons are intelligently connected even without external input.

Several studies have indicated that neurons have a well-established system of highly nonlinear ionic currents and synaptic dynamics [11]. However, a single neuron only exhibits chaotic behavior when exposed to external stimuli, a behavior quite different from the intact brain. According to previous studies, goal-directed behaviors cannot be effectively modeled without including the chaotic behavior that occurs at the mesoscopic level [9]. Our experiments indicated that a cultured cell model did not always spontaneously manifest chaotic behavior. In four long-term cultures (more than three months *in vitro*), chaotic behavior was only observed after about 4–9 weeks *in vitro*. When there were few active sites, random spiking appeared in the spontaneous activity rather than chaotic firing. We inferred that the existence of chaos would indicate maturity, which was different from the previous studies [15,18,46]. More importantly, we found that the largest Lyapunov exponent of the entire network depended on the number of active neurons (Fig. 7 demonstrated positive correlation between them). This finding suggested that chaotic behavior emerged from the self-organized interaction between cells *in vitro*, a fact critical to understanding the emergence of intentional states from the interactive dynamics of multiple neurons [9,10].

Our results also provided experimental evidence for Lipsitz and Goldberger's theory [47,48] that a change in the complexity of a biological system results from a change in either the number of individual structural components or the coupling function between the components. The relation between chaotic dynamics and neural development will be investigated in a future study using more long-term MEA cultures.

It has been suggested that chaos control may be useful in the therapy of neurological diseases [7]. However, the application of chaos within the human body has many limitations and unknown dangers. Cultured networks on multielectrode arrays have provided effective models that can be used with electrical stimulation or pharmacological experiments [49]. The present study could shed light into chaos control. To encourage further studies on chaotic behavior using cultured networks, we wish to make our data available to researchers around the world.

## ACKNOWLEDGMENTS

This work was supported by the National Natural Science Foundation of China (Grants No. 30727002 and No. 30800314). The authors thank Professor Xiaosong Yang, Shaoqun Zeng, Hui Gong, and Wei Zhou for valuable discussions and two reviewers for their constructive comments that were critical to improve this paper.

[1] G. Laurent, M. Stopfer, R. W. Friedrich, M. I. Rabinovich, A. Volkovskii, and H. D. I. Abarbanel, Annu. Rev. Neurosci. **24**, 263 (2001).
[2] E. M. Izhikevich and G. M. Edelman, Proc. Natl. Acad. Sci. U.S.A. **105**, 3593 (2008).
[3] S. Fujisawa, M. K. Yamada, N. Nishiyama, N. Matsuki, and Y. Ikegaya, Biophys. J. **86**, 1820 (2004).
[4] O. Darbin, J. Soares, and T. Wichmann, Brain Res. **1118**, 84 (2006).
[5] D. Durstewitz and T. Gabriel, Cereb. Cortex **17**, 894 (2007).
[6] H. Kantz and T. Schreiber, *Nonlinear Time Series Analysis* (Cambridge University Press, Cambridge, 2004).
[7] S. J. Schiff, K. Jerger, D. H. Duong, T. Chang, M. L. Spano, and W. L. Ditto, Nature (London) **370**, 615 (1994).
[8] P. Faure and H. Korn, C. R. Acad. Sci. III **324**, 773 (2001).
[9] W. J. Freeman, *Neurodynamics: An Exploration in Mesoscopic Brain Dynamics* (Springer, London, 2000).
[10] I. Tsuda, Chaos **19**, 015113 (2009).
[11] H. Korn and P. Faure, C. R. Biol. **326**, 787 (2003).
[12] I. Franovic and V. Miljkovic, Phys. Rev. E **79**, 061923 (2009).
[13] W. J. Freeman, J. Physiol. Paris **94**, 303 (2000).
[14] S. Marom and G. Shahaf, Q. Rev. Biophys. **35**, 63 (2002).
[15] D. A. Wagenaar, J. Pine, and S. M. Potter, BMC Neurosci. **7**, 11 (2006).
[16] D. A. Wagenaar, Z. Nadasdy, and S. M. Potter, Phys. Rev. E **73**, 051907 (2006).
[17] J. M. Beggs and D. Plenz, J. Neurosci. **24**, 5216 (2004).
[18] J. van Pelt, P. S. Wolters, M. A. Corner, W. L. Rutten, and G. J. Ramakers, IEEE Trans. Biomed. Eng. **51**, 2051 (2004).
[19] F. Esposti, M. G. Signorini, S. M. Potter, and S. Cerutti, IEEE Trans. Neural Syst. Rehabil. Eng. **17**, 364 (2009).
[20] E. Fuchs, A. Ayali, A. Robinson, E. Hulata, and E. Ben-Jacob, Dev. Neurobiol. **67**, 1802 (2007).
[21] T. Tateno, A. Kawana, and Y. Jimbo, Phys. Rev. E **65**, 051924

(2002).
[22] R. Segev, M. Benveniste, E. Hulata, N. Cohen, A. Palevski, E. Kapon, Y. Shapira, and E. Ben-Jacob, Phys. Rev. Lett. **88**, 118102 (2002).
[23] X. Li, W. Zhou, S. Zeng, M. Liu, and Q. Luo, Biosens. Bioelectron. **22**, 1538 (2007).
[24] W. Zhou, X. Li, M. Liu, Y. Zhao, G. Zhu, and Q. Luo, BioSystems **95**, 61 (2009).
[25] G. Shahaf and S. Marom, J. Neurosci. **21**, 8782 (2001).
[26] E. N. Brown, R. E. Kass, and P. P. Mitra, Nat. Neurosci. **7**, 456 (2004).
[27] S. K. Mistry, E. W. Keefer, B. A. Cunningham, G. M. Edelman, and K. L. Crossin, Proc. Natl. Acad. Sci. U.S.A. **99**, 1621 (2002).
[28] A. Babloyantz and A. Destexhe, Proc. Natl. Acad. Sci. U.S.A. **83**, 3513 (1986).
[29] M. T. Rosenstein, J. J. Collins, and C. J. D. Luca, Physica D **65**, 117 (1993).
[30] D. Zhou, A. V. Rangan, Y. Sun, and D. Cai, Phys. Rev. E **80**, 031918 (2009).
[31] T. Schreiber and A. Schmitz, Physica D **142**, 346 (2000).
[32] A. Mokeichev, M. Okun, O. Barak, Y. Katz, O. Ben-Shahar, and I. Lampl, Neuron **53**, 413 (2007).
[33] T. Schreiber and A. Schmitz, Phys. Rev. E **55**, 5443 (1997).
[34] S. Shinomoto, K. Shima, and J. Tanji, Neural Comput. **15**, 2823 (2003).
[35] N. Marwan, M. C. Romanoa, M. Thiela, and J. Kurths, Phys. Rep. **438**, 237 (2007).
[36] I. Vajda, J. van Pelt, P. Wolters, M. Chiappalone, S. Martinoia, E. van Someren, and A. van Ooyen, Biophys. J. **94**, 5028 (2008).
[37] G. Innocenti, A. Morelli, R. Genesio, and A. Torcini, Chaos **17**, 043128 (2007).
[38] M. A. Fitzurka and D. C. Tam, Biol. Cybern. **80**, 309 (1999).
[39] I. Tsuda and H. Fujii, J. Integr. Neurosci. **6**, 309 (2007).
[40] L. Korbo, B. Pakkenberg, O. Ladefoged, H. J. Gundersen, P. Arlien-Soborg, and H. Pakkenberg, J. Neurosci. Methods **31**, 93 (1990).
[41] L. M. A. Bettencourt, G. J. Stephens, M. I. Ham, and G. W. Gross, Phys. Rev. E **75**, 021915 (2007).
[42] T. Sasaki, N. Matsuki, and Y. Ikegaya, J. Neurosci. **27**, 517 (2007).
[43] I. Tsuda, Behav. Brain Sci. **24**, 793 (2001).
[44] G. Tanaka, B. Ibarz, M. A. Sanjuan, and K. Aihara, Chaos **16**, 013113 (2006).
[45] M. A. Komarov, G. V. Osipov, and J. A. Suykens, Chaos **18**, 037121 (2008).
[46] J. van Pelt, I. Vajda, P. S. Wolters, M. A. Corner, and G. J. A. Ramakers, Prog. Brain Res. **147**, 171 (2005).
[47] L. A. Lipsitz and A. L. Goldberger, JAMA, J. Am. Med. Assoc. **267**, 1806 (1992).
[48] D. E. Vaillancourt and K. M. Newell, Neurobiol. Aging **23**, 1 (2002).
[49] P. L. Baljon, M. Chiappalone, and S. Martinoia, Phys. Rev. E **80**, 031906 (2009).